*Russian Chemical Reviews* **70** (2) 147 – 159 (2001) © 2001 Russian Academy of Sciences and Turpion Ltd

DOI 10.1070/RC2001v070n02ABEH000637

# Metallic nanosystems in catalysis

V I Bukhtiyarov, M G Slin'ko

## Contents


| | | |
|---|---|---|
| I. | Introduction | 147 |
| II. | Physicochemical properties of nanostructures | 147 |
| III. | Reactivities and catalytic properties of nanostructures | 150 |
| IV. | The prospects for the application of nanostructures in catalytic processes | 154 |
| V. | Conclusion | 157 |


**Abstract. The reactivities of metallic nanosystems in catalytic processes are considered. The activities of nanoparticles in catalysis are due to their unique microstructures, electronic properties and high specific surfaces of the active centres. The problems of increasing the selectivities of catalytic processes are discussed using several nanosystems as examples. The mutual effects of components of bimetallic nanoparticles are discussed. The prospects for theoretical and experimental investigations into catalytic nanosystems and the construction of industrial catalysts based on them are evaluated. The bibliography includes 207 references.**

## I. Introduction

Metallic catalysts supported on various carriers (*e.g.*, $SiO_2$, α- and γ-$Al_2O_3$, zeolites, magnesium and chromium oxides, carbonaceous materials, *etc*.) are widely employed in chemical, petrochemical and oil-refining industries as well as for purification of gaseous industrial wastes and motor transport exhausts from toxic components. The production of efficient industrial catalysts includes selection of inert carriers of definite porous structures, their coating with particles of active metals of predetermined compositions, sizes and structures and the most efficient unimodal distribution of these particles over the carrier surface.

Catalytic reactions occurring on the catalyst's surface consist in adsorption of molecules of the starting compounds, their migrations, chemical conversions of adsorbed substances and subsequent desorption of the products formed. The gas-phase components are dissolved in the near-surface layers of the catalyst thus changing its reactivity. In some cases where a certain degree of coating of the catalyst's surface with the adsorbed molecules is achieved, its spontaneous and adsorption-induced reconstruction takes place. The energies of lateral interactions of the adsorbed species, their mobilities and the energies of binding of the interacting molecules to the catalyst are the crucial factors which determine the rates of the elementary catalytic steps mentioned above. The efficiency of a catalyst depends on how fast and concertedly do the active sites on the catalyst's surface adsorb the reacting species, retain them during the chemical conversions and liberate the reaction products to be recovered for the next catalytic cycle. The maximum reaction rate is reached when the adsorption, reaction and desorption possess the optimum energies of binding of molecules to the catalyst (the Sabatier – Balandin principle).

The rates of individual elementary stages depend differently on the size of the active metal particles; hence, the total rate of the reaction varies with a change in the particle size. The knowledge of the structure and properties of the active sites and their distribution over the catalyst's surface is of primary importance for establishing a correlation between the structure and properties of the catalyst's surface and the particle size. It is also desirable to establish the number of adsorbed reacting species and metal atoms involved in an elementary catalytic act.

**V I Bukhtiyarov** G K Boreskov Institute of Catalysis, Siberian Branch of the Russian Academy of Sciences, prosp. Akad. Lavrent'eva 5, 630090 Novosibirsk, Russian Federation. Fax (7-383) 234 37 66. Tel. (7-383) 234 17 71. E-mail: vib@catalysis.nsk.su
**M G Slin'ko** State Scientific Centre of the Russian Federation 'L Ya Karpov Institute of Physical Chemistry', ul. Vorontsovo Pole 10, 103004 Moscow, Russian Federation. Fax (7-095) 975 24 50. Tel. (7-095) 917 78 70. E-mail: slinko@polymer.chph.ras.ru

Received 20 November 2000
*Uspekhi Khimii* **70** (2) 167 – 181 (2001); translated by R L Birnova

## II. Physicochemical properties of nanostructures

The intermediate position occupied by nanoparticles between the metals in bulk and individual atoms predetermines the deviation of their physicochemical properties from those of bulk metals, on the one hand, and those of isolated atoms, on the other hand. Such characteristics of nanoparticles with the sizes ranging from several tens to units of nanometres are affected as the electronic, magnetic, optical properties and many others. The changes in the surface structures and electronic properties of metallic nanoparticles present the greatest interest for specialists in catalysis, because these characteristics determine primarily specific interactions of the reactants with the surface of the active component, the nature and reactivities of the adsorbed species and eventually the activities and selectivities of the nanosystems in heterogeneous catalysis.

### 1. The structure and geometry of the surface

The atoms inside bulk crystals have optimum chemical bonds with all adjacent atoms. If the number of metal atoms in the particle ($N$) is less than 13, it has a close packing in which each atom represents a surface atom. For $N \geqslant 13$, two kinds of atoms exist, *viz*., the inner and surface ones. The proportion of surface atoms in a cluster † depends on the total number of atoms.

† Many investigators believe that in contrast to particles, clusters comprise a strictly definite number of atoms and thus represent nearly monodisperse structures with sizes less than 10 nm.

| | | | | | |
|---|---|---|---|---|---|
| Number of atoms in a cluster | 13 | 55 | 147 | 349 | 561 |
| Proportion of surface atoms (%) | 92 | 76 | 63 | 52 | 45 |

These data refer to clusters with 'shell' structures which are characterised by close packing of their metal atoms (see below). For $N = 13$, such clusters have only one inner layer (consisting of only one atom, whereas for $N = 55$ and $N = 147$, these have two and three inner layers of atoms, respectively. Then, the particle size increases from 0.8 to 2 nm. In particles with sizes of 2–10 nm, the numbers of surface and inner atoms are comparable, whereas in particles with sizes > 30 nm the fraction of surface atoms is less than 2%. Hence, the proportion of surface atoms decreases with an increase in the particle size, their coordination properties with respect to the reactants change too. Small particles form many different faces; their number and parameters depend on the method used for their preparation. The properties of the particles approach those of bulk crystals with an increase in the particle size.

The surface structures of metallic particles are studied by theoretical and experimental methods.[1–4] The theoretical approach is based on the analysis of the equilibrium form of crystals [1] determined by the minimum value of Gibbs' free energy. The total energy depends on the thermodynamic properties of the bulk phases, the contribution of the planar surface and the plane intersection energy, which corresponds to the contribution of curved or rough surfaces. Obviously, the surface structures of nanoparticles are determined by the ratio of contributions of planar and rough surfaces, which in turn depends on the particle size. For large particles, the contribution of rough surfaces is insignificant and the equilibrium form of a crystal is determined by the minimum surface energy. The contribution of the curved surface increases with a decrease in the particle size. Hence, the surface of nanoparticles contains predominantly planar, planar and rough or predominantly rough areas depending on their sizes.

Experimental studies of surface structures are complicated, since the methods employed should ensure resolution at the atomic level. Transmission electron microscopy (TEM) is one such method. Studies of nanoparticles using TEM corroborated the presence of planar and rough surface areas and made it possible to follow their alterations with a change in the nanoparticle size.[3,4] Thus a combination of TEM with computer simulation of surface structures showed that the surface of platinum particles (~ 8 nm) consists of (111) faces (~ 37%), (100) faces (28%) and rough areas (35%).[4] It is noteworthy that the rough areas contain faces with higher Miller's indices, *e.g.*, (001), (113), (012) and (133) faces. The results of computer simulation studies of rough areas and of platinum particles as a whole are presented in Fig. 1.

In recent years, scanning tunnelling microscopy (STM), which ensures resolution at the atomic level, has been widely used for the study of surface structures of metallic nanoparticles.[5–9] It was found that surface structures of small (1–2 nm) metallic particles are determined by their shapes which in turn strongly depend on the nature of the support. At the same time, such low coordinated sites as edges and kinks strongly affect the interaction of a surface with adsorbed species. The use of STM for the analysis of surface structures of metallic nanoparticles seems promising, since in contrast to TEM this method allows *in situ* analysis of surface structures, *i.e.*, in the course of a catalytic reaction.

An alternative procedure is based on the adsorption of molecules the spectral characteristics of which are sensitive to the structure of the adsorption centre. Successful application of this method entails the choice of a suitable molecular probe and measurements of its spectral characteristics in the adsorption on single crystals with different surface structures. Like STM, this method permits one to obtain information *in situ*, which is extremely important in studies of catalytic reactions, especially those where the molecular probe is one of reactants. NMR and IR spectroscopic studies of CO adsorption on platinum and palladium clusters supported on $SiO_2$ is an example.[10–12] It was shown

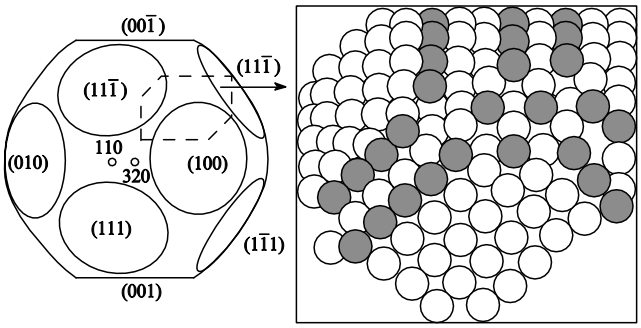



**Figure 1.** The types of faces on the surface of a platinum particle (8 nm) and a structural model of a site marked by a dashed line.[4] The light and dark circles designate the atoms localised at different levels.

that part of the $^{13}CO$ is adsorbed on platinum catalysts in a linear rather than a bridge-like form, the proportion of the linear fraction being increased with an increase in the degree of platinum dispersion from 16%–19% to 56%.[10] This effect was attributed to the fact that the surfaces of smaller platinum particles contain more low-coordinated sites. A similar conclusion was made by Xu *et al.*[11] who showed that the major part of the CO is adsorbed on small palladium particles in a linear rather than in a bridge-like form. This points to a higher concentration of defect/edge sites in small nanoparticles in comparison with large ones.

An analysis of spectra of the O 1*s* core level recorded after low-temperature adsorption of $O_2$ was proposed by us for investigation of surface structures of supported silver. This approach is based on the previously established regularity, *viz.*, the greater the number of defects on the silver surface the lower the minimum temperature needed for dissociation of oxygen molecules.[13–15] In other words, the amount of atomic oxygen after low-temperature adsorption correlates with surface defects of the supported silver particles. Studies of low-temperature ($T = 140$ K) adsorption of $O_2$ on silver particles deposited onto a graphite surface revealed that the form (atomic or molecular) of the chemisorbed oxygen depends on the sizes of the silver particles. The molecular form is absent in the case of small (< 10 nm) particles which suggests a high degree of defectiveness of their surface structures, while this is present with an increase in the particle sizes to 20–40 nm. The latter circumstance points to the formation of (111) and (110) low-index faces. It is worth noting that the dimension-dependent effect is manifested in the epoxidation of ethylene on silver catalysts in the range of particle size from 40 to 50 nm.

These data altogether suggest that the surfaces of small clusters do not exclusively contain low-index faces, such as (111), (110) or (100) faces. The greater part of the surface, which increases with a decrease in the nanoparticle size, is occupied by curved areas. This circumstance is of crucial importance for the catalysis by nanoparticles, since the adsorption properties of rough surface defects (*e.g.*, angles, steps, edges, *etc.*) differ from those of flat surfaces. Therefore, simple extrapolation of experimental data obtained for single crystals to real catalytic systems is impossible. In this connection, studies of reactivities of metallic nanoparticles become especially urgent.

## 2. Electronic properties

As the number of atoms in nanoparticles is limited, their electronic structures occupy an intermediate position between the discrete energy levels of free atoms and continuous energy bands of the bulk metal. The dependence of electronic structures of metallic particles on their sizes was studied in particular by Kubo,[16] who suggested that the spectrum of the energy levels of nanometre particles should resemble that of a large molecule rather than that of a bulky solid. The electronic levels of atoms in a large metallic particle are close to one another and eventually overlap to form energy bands. The expression:

$$h = \frac{E_F}{N}, \quad (1)$$

where $E_F$ is the Fermi level energy and $N$ is the number of atoms in a metallic particle, was proposed to evaluate the distance between the neighbouring energy levels ($h$). Estimation of the maximum size of a particle where changes in its electronic properties can occur as calculated by this simple formula gives the value of $\sim 2$ nm. Presumably, this is the threshold size where significant changes in the electronic properties of supported metallic nanoparticles are observed. This hypothesis was confirmed by experimental data. It was found that the properties of nanoparticles change so drastically in the size range of 2–5 nm that a 'metal–non-metal' transition becomes very likely. This conclusion is based on the increase in the binding energy of electrons ($E_b$) at core levels [16] [the binding energy was measured by X-ray photoelectron spectroscopy (XPS)] with a decrease in the sizes of metallic nanoparticles.

In the general case, the changes in $\Delta E_b$ are due to the contribution of the following terms:

$$\Delta E_b = \Delta E + \Delta E_R + \Delta E_F, \quad (2)$$

where $\Delta E$ is the 'true chemical shift' equal to the difference between the energies of different initial states of the element under study,‡ $\Delta E_R$ is the change in the relaxation energy and $\Delta E_F$ is the difference between the Fermi level energies.

The last two terms in equation (2) are determined by the effects of the final state as a result of photoelectron emission, *viz*., the $\Delta E_R$ value reflects the changes in the relaxation energy upon the screening of photoelectron vacancies caused by redistribution of electrons in the solid, whereas $\Delta E_F$ reflects possible changes in the Fermi level of a sample relative to that of the spectrometer.§ If the conductivity of the sample is high enough, an electrochemical equilibrium is established between the sample and the spectrometer. In this case, the positive charge induced by photoelectron emission is neutralised due to the transition of electrons from the 'earth' to the sample and the contribution of $\Delta E_F$ to the total change in $\Delta E_b$ will be insignificant. If the electronic conductivity of the sample is not high enough to compensate for the charge due to photoemission, the positive charge is accumulated on the surface of the sample. The electrons passing through this positively charged layer lose their kinetic energies, which results in the overestimation of the apparent binding energy. This suggests that the Fermi levels of the sample and the spectrometer are no longer at equilibrium, which results in the charging effect due to accumulation of unknown surface potential.

The subdivision into terms proved to be useful for establishing the reasons for the change in $\Delta E_b$ with a decrease in the metallic nanoparticle sizes. It was suggested (see, *e.g*., Refs 17 and 18) that it is the relaxation effect that underlies the positive shift of the binding energy in small metallic nanoparticles (2–3 nm) by 0.5–1.0 eV in comparison with the binding energy of the bulk metal. However, studies of alloys [19,20] and those employing isochromatic spectroscopy [21,22] revealed that the observed shift in the binding energy cannot be attributed to the relaxation effect alone. It was concluded that the changes in the initial state of atoms in metal clusters with particle sizes of less than 2–3 nm are due to the 'metal–non-metal' transition. This conclusion is of fundamental importance, since the changes in the initial states of atoms in small clusters should influence (and they do influence, as will be shown below) their reactivities with respect to the gases to be adsorbed. It is evident that the catalytic properties of clusters cannot remain unchanged under these conditions.

In contrast to the initial-state and relaxation effects, the contribution of the charging effect to total changes in $\Delta E_b$ was not taken into consideration by the majority of authors who dealt with studies of electronic properties of metal clusters. Such an approach is justified with respect to homogeneous insulator specimens where the magnitude of the charging potential is identical for all inner levels and can be easily taken into consideration in the analysis of XPS spectra by the internal standard method. The situation is more complicated in heterogeneous systems where different phases are characterised by different conductivities. In this case, the surface charges are different in individual phases of the specimen, which generates the so-called differential charging of the more conducting phase in comparison with the less conducting one. Apparently, this situation is quite realistic in the case of heterogeneous catalysts which contain metallic nanoparticles supported onto the surface of dielectric substrates ($Al_2O_3$, $SiO_2$, *etc*.). Indeed, it was demonstrated [23,24] that metallic crystallites with the sizes ranging from five to several tens of nanometres manifest the properties of conducting metals by providing more efficient compensation of the surface charge in comparison with the surface of insulating substrates. As a result, the charge potential on metallic particles is lower than that of the dielectric substrate, and the corresponding lines of the substrate in the XPS spectra manifest a greater shift in the binding energy ($\Delta E_b$) than those of the supported metal. Then, the shift of the spectra by a value equal to the charge of the substrate, the lines of which are generally used as internal standards in calibration of XPS spectra, will produce an apparent negative shift in the lines of the corresponding spectra of the metals.

The latter effect is manifested exclusively upon photoemission; however, it can be of tremendous importance for characterisation of reactivities of various particles including silver particles. The hypothetical role of the conductivity electrons in the formation of chemical bonds between the metal surface and chemisorbed molecules which was put forward as early as 1937,[25] was corroborated later by quantum-chemical calculations.[26] The role of the conductivity electrons in the formation of chemical bonds was confirmed experimentally by the presence of the Knight shift in the $^{13}C$ NMR spectra of carbon oxide adsorbed on supported metallic particles.[27,28]

The effects of differential charging can be taken into account with the help of those parameters of XPS spectra which do not depend on the surface charge. One of them is the modified Auger parameter $\alpha$, which represents the sum of the binding energies of the most intense line in the XPS spectrum of the element under study and the kinetic energy of the corresponding Auger peak.[29] Since the charge potential increases the binding energy of the core level and decreases the corresponding kinetic energy of the Auger peak by the same value, their sum is not changed with changes in the charge. With the use of the Auger parameter we have demonstrated that it is the differential charging of supported nickel and silver particles that is responsible for the changes in the binding energies of their core levels ($2p_{3/2}$ and $3d_{5/2}$, respectively) in catalysts (both fresh and treated with the reaction mixture) for butadiene hydrogenation (Ni/C) and ethylene epoxidation (Ag/$Al_2O_3$).[30–32]

Treatment of nickel particles supported onto carbon filaments with the reaction mixture causes a shift in the overall Ni spectrum ($2p_{3/2}$) by 1.1 eV towards higher values of $E_b$ with a simultaneous decrease in the Ni : C ratio.[30] The constancy of the parameter $\alpha$ and the absence of a shake-up satellite in the Ni $2p_{3/2}$ spectrum indicate that both fresh and treated samples contain metallic nickel, whereas the shift in the Ni spectrum $2p_{3/2}$ is due to the differential charging.

Studies of $Ag/Al_2O_3$ catalysts where the sizes of silver particles vary from 10 to 100 nm revealed a negative shift in the Ag $3d_{5/2}$ spectra by 0.3–0.4 eV for particles with the sizes above 50 nm.[31,32] In this case, the parameter $\alpha$ was constant for all

‡ The XPS method owes its second name which is widely used by researchers *viz*., 'electron spectroscopy for chemical analysis' (ESCA), to the term $\Delta E$.

§ 'The Fermi level of spectrometer' is a popular term used to define the Fermi level of the material (mostly, gold) of which the energy analyser of the spectrometer is made.

specimens and equal to 726.2 eV. Comparison of this parameter with the known values of $\alpha$ for metallic silver (726.0 – 726.3 eV) and silver oxides (724.0 – 724.5 eV) suggests that the samples under study contain particles of metallic silver. This conclusion was confirmed by the results of an X-ray phase analysis and scanning tunnelling microscopy, which have demonstrated the presence of the $\alpha$-$Al_2O_3$ phase and metallic silver in the specimens.[33]

The observed change in $E_b$(Ag $3d_{5/2}$) is determined by the effect of a differential charging of the supported silver, which in turn is due to the inner conductivity of large silver particles and the lack of conductivity of the surface of the non-conducting substrate.[31] This conclusion is in good agreement with the results of NMR studies of silver catalysts[34,35] according to which the Knight shift of the $^{147}$Ag signal disappears if the size of silver particles is less than 50 nm. Since the Knight shift is determined by hyperfine interactions of silver nuclei with the conductivity electrons, it is clear that the size of several tens of nanometres is critical with respect to the conductivities of supported silver particles. The great importance of such changes in the properties of silver conductivity electrons for catalysis is illustrated in Fig. 2. As can be seen, the rate of ethylene epoxidation decreases more than 10-fold with a decrease in the sizes of silver particles below 50 nm. It will be shown below that this correlation depends on the form of oxygen adsorbed on silver.

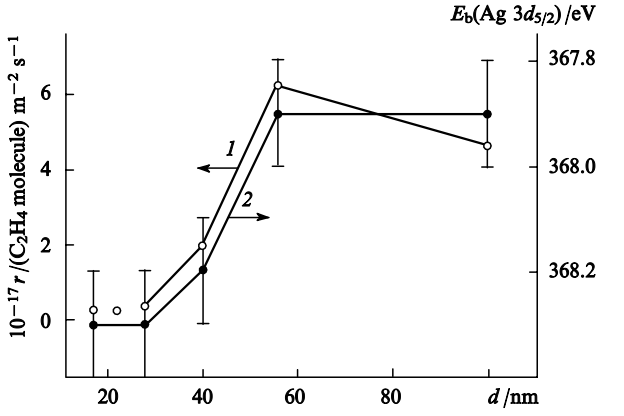



**Figure 2.** The dependence of the rate of ethylene epoxidation (*1*) and the binding energy $E_b$(Ag $3d_{5/2}$) (*2*) on the average size of silver particles in non-promoted $Ag/Al_2O_3$ catalysts.

A correlation was also found[36–38] between the deviation of electronic properties of supported nanoparticles from those of bulk metals and the catalytic activities of nanoparticles.

## III. Reactivities and catalytic properties of nanostructures

The existence of size effects in electronic and structural properties of nanostructures implies that their reactivities with respect to gaseous molecules also differ from those of bulk metals, this difference being more pronounced in smaller particles. The first evidence for such dependence was obtained in catalytic studies which demonstrated that the rates of numerous reactions catalysed by metallic nanoparticles vary in the same range[39] as their electronic and structural properties.[10–12,19–21,40–42] Catalytic reactions usually occur on the catalyst's surface. Therefore, the activities of catalysts are conventionally referred to unit surface area. This quantity, which is termed 'specific catalytic activity' (SCA), is determined by the chemical composition, sizes of crystallites, structures of surface faces, structural irregularities and miscellaneous defects. Therefore, the knowledge of changes in the catalytic properties of the catalyst's surface caused by changes in both the sizes of crystallites and surface structures of their faces is of fundamental importance for the theory and practice of catalysis. Although the structures of nanocrystals can differ from those of macroscopic crystals due to exposure of other types of faces on their surface,[43] we thought it appropriate to analyse, at least briefly, the results of investigations of applied single crystals with different surface orientations as the subjects. This is especially important, because the results of such studies are very often used as references for illustrating the dependence of reactivities of metallic nanoparticles on their sizes, as will be shown below.

### 1. The reactivities and catalytic properties of single crystal faces

The properties of atoms in the crystal lattices of metals are determined by their specific atomic environment, *i.e.*, the number of adjacent and more remote neighbours, and the sizes of the corresponding coordination zones. Therefore, the reactivity of a surface depends essentially on the localisation of atoms on one or another crystallographic face and the parameters of their atomic environment. A correlation between the orientation of the crystal faces and their catalytic activities was established by A A Balandin as early as 1929.[44] In the past years, the number of investigations of this kind has increased manifold.

The rates of carbon monoxide oxidation on (111), (100), (410) and (210) faces of the single crystal $Pt_{0.25}Rh_{0.75}$ at different temperatures, total pressure of $2 \times 10^{-7}$ mbar and the $CO:O_2$ ratio of 2 : 1 differ markedly.[45] On heating, the reaction rates on different planes increase rapidly but differently in the range of 400 – 500 K and then decrease slowly after reaching a certain maximum. The higher the strength of lateral interactions of the CO molecules, the higher the temperature at which the maximum rate is achieved. The oxidation of CO on the faces of Pt, Pd, Ir, Rh and Ru crystals proceeds in a similar way.

The catalytic activity of the (111) face of iron in the synthesis of ammonia from nitrogen and hydrogen is about 430 times higher than that of the closely packed (110) face and 13 times higher than that of the (100) face.[46] It is also known that aromatisation and cyclisation of hydrocarbons occur on the (111) face of platinum, whereas the (100) face is responsible for their isomerisation and hydrogenolysis. The presence of curved areas, *e.g.*, (10 8 7) favours the formation of undesired products, such as propane and ethane.

The atoms in the surface layer can be at equilibrium with the atoms in the second layer. Since the bonds of the surface atoms are not compensated, their equilibrium positions can differ from their positions in the bulk. Such 'surface reconstruction' was observed in the CO oxidation catalysed by platinum and some other metals. For example, the reaction occurring on the (110) face of platinum single crystals is accompanied by spontaneous reconstruction of the surface from the $(1 \times 1)$ state into the $(1 \times 2)$ state. Surface rearrangements are due to interactions between the platinum atoms, CO molecules and oxygen atoms.[47–49] The higher reactivity of the (110) face of platinum in comparison with other faces can be the reason for autooscillations of the reaction rate.[48–54] On this face, spatial-temporal self-organisation in the form of progressive spiral and stationary reaction waves and chaotic regimes were observed in the nano- and micrometre ranges. On the other hand, the oxidation of carbon monoxide by oxygen on the (111) face of platinum at low partial pressures of CO and $O_2$ and at 300 – 700 K was unaccompanied by changes in the surface structure and, correspondingly, by autooscillations of the reaction rate.

The activation energy of a catalytic reaction depends on the coverage of the catalytic surface with oxygen and carbon monoxide.[47] The adsorbed oxygen atoms increase the reaction rate, while adjacent CO molecules decrease it. The distribution of atoms and molecules adsorbed on the surface of a catalytic species influences substantially the dependence of the rates of elementary stages of the catalytic reaction on the degree of coverage of the catalytic surface.

Spatial-temporal self-organisation was also observed in a nanometre range in the interaction of NO and $H_2$ on the (110) face of rhodium single crystals at partial pressures of nitrogen

oxide and hydrogen of $10^{-6}$–$10^{-4}$ mbar and at temperatures on the catalyst's surface of 300–800 K.[55–58] Phase transitions of the 'order–disorder' type and various superstructures of adsorbed hydrogen atoms were found. The nitrogen atoms initiated the rearrangement of the original surface resulting in the appearance of the $(3 \times 1)$–N superstructure recorded by low energy electron diffraction. This was transformed into the $(2 \times 1)$–N superstructure with an increase in the degree of coverage of the catalyst's surface with the adsorbed nitrogen.[59] Lateral interactions of adsorbed particles and their mobilities exert a crucial effect on the formation of structures on a nanometre range. The NO + $H_2$ system on Rh(110) was also characterised by anisotropy of the near-surface layer and the presence of unusual reaction autowaves of different shapes. Non-linear phenomena, *e.g.*, spatial-temporal self-organisation in nanosized particles, significantly influence both the spatial structure of the reaction autowaves at the meso level and the rate of the catalytic reaction.

The effects of the structural factor on SCA can also be explained by assuming that the surface of small metallic clusters contains many more low-coordinated atoms than that of bulk metals.[60] Indeed, the proportion of surface atoms, particularly those localised in the apices as well as on the boundaries and faces and characterised by lower coordination numbers than atoms localised inside the crystals, increases essentially in crystallites the sizes of which exceed 5 nm. If this is true, SCA will depend on the changes in the crystallite sizes in the range of not more than 1–5 nm, whereas the catalytic activities of larger crystallites will be determined by the structures of the faces exposed on the surface of the nanoparticles.

## 2. The reactivities and catalytic activities of nanostructures

The first attempts to establish a correlation between the rate of a catalytic reaction and the particle size of the active component were undertaken by Kobozev in the late 1930's.[61] These investigations were continued in the early 1950's by Boreskov *et. al.*[62, 63] who have formulated a rule of relative stability of SCA of catalysts having identical chemical compositions. A similar conclusion was made later by Boudart *et al.*[64, 65] who have named this kind of reaction 'structure-insensitive reactions'. However, the rates of many reactions do depend on the degree of dispersion of the active component, and these reactions have been named 'structure-sensitive reactions'. Further studies of the dependence of catalytic activities of metals on the particle size have revealed [66–76] that all metal-catalysed reactions can be classified into four main groups, *viz.*,

(a) SCA depends only weakly on the size of the supported metal particles (structure-insensitive reactions);

(b) SCA drops with a decrease in the particle size (the so-called negative size effect);

(c) SCA increases with a decrease in the particle size (the positive size effect);

(d) maximum SCA is characteristic of particles of intermediate sizes.

Seemingly, in the case of structural insensitivity or a positive dimensional effect the sizes of nanoparticles of the active component in certain systems can be minimised, thus affecting favourably the economical parameters of the industrial process. Unfortunately, this assumption was refuted by some examples.[77, 78] It was shown [77] that the rate of even such structure-insensitive reactions as the hydrogenation of hydrocarbons decreases by more than two orders of magnitude in those cases where iridium nanoclusters ($d \approx 2$–$3$ nm) supported on MgO were used instead of conventional Ir/MgO catalysts, whereas the tenfold increase in the activity of the $Ir_n/\gamma$-$Al_2O_3$ catalyst in the hydrogenation of toluene is explained [78] by the formation of iridium agglomerates during the annealing of fresh samples in hydrogen at 573 K.[78]

Obviously, such drastic differences in the behaviour of SCA as a function of the particle size are due to changes in the reactivities of the particles with respect to the participants of the catalytic reaction. This accounts for a great number of publications devoted to the analysis of reactivities of nanoparticles. However, real specimens used in catalytic studies appeared to be unsuitable subjects for establishing an exact correlation between the changes in the catalytic properties and reactivities. Progress in this field could be achieved, if model systems were used. These were prepared by covering flat samples of a substrate with metal particles using physical (*e.g.*, deposition of bulk metals in high vacuum) or chemical methods (*e.g.*, introduction of chemical compounds of a metal followed by reduction and/or calcination).

For the first time, the reactivities of metallic clusters were studied in detail using the oxidation of CO on platinum metals as an example.[79–82] This choice has been made owing to the large body of experimental material obtained in precision studies of this reaction on bulk metals.[83–86] These results could be used for the analysis of reactivities of nanostructures supported on metals.

Thus the earlier established mechanism of this reaction carried out on the (111) face of palladium [83] was used to explain the peculiarities of CO oxidation on palladium clusters supported on $\alpha$-$Al_2O_3$.[79, 80] The threefold increase in the rate of $CO_2$ formation at temperatures > 500 K upon a decrease in the sizes of palladium clusters from 4.9 to 1.5 nm was attributed to the increased coefficient of CO adhesion to edge and corner palladium atoms the number of which increases with a decrease in the particle size.[79] This explanation was corroborated by experiments [87] in which the reactivities of palladium clusters with respect to CO were studied by temperature-programmed desorption (TPD). It was shown that the TPD spectra of CO molecules adsorbed on palladium with the particle size of 27 nm and on the (111) face of palladium single crystals coincide, whereas the corresponding spectra of desorption of CO with a particle size of 2.5 nm display an additional peak at lower temperatures. Similar TPD spectra were recorded by following the CO desorption from palladium with a particle size of < 5 nm supported on mica. This suggests that the formation of weakly bound forms of carbon monoxide is characteristic of small palladium particles and does not depend on the nature of the substrate.[88] Presumably, it is the appearance of a weakly bound adsorbed form of CO that is responsible for the increased rate of $CO_2$ formation with a decrease in the sizes of palladium nanoparticles.[79, 80]

Quite opposite regularities were observed by following the temperature-programmed desorption of CO molecules from platinum particles supported on $Al_2O_3$ (Ref. 89) and mica (Ref. 90), *viz.*, the intensity of the low-temperature peak of the CO desorption decreased with a decrease in the size of the platinum particles (> 4 nm). It was thus concluded that CO molecules are more strongly adsorbed on small particles, which can account for the decrease in the rate of CO oxidation on small (< 2.5 nm) platinum particles.[81]

Comparison of CO adsorption on supported platinum and rhodium particles revealed that the ratio of low- and high-temperature components in the TPD spectra of rhodium particles (in contrast to the corresponding parameters in the TPD spectra of platinum particles), only weakly depends on the size of the metal particles.[91] Presumably, this peculiarity of CO adsorption on rhodium is the reason for the structure-insensitivity of the CO oxidation on Rh-containing catalysts.[82]

These data suggest that a correlation exists between catalytic activity in the CO oxidation on various platinum metals and the strength of the CO–metal bond despite significant differences in the manifestations of the size effect. The fact that the structure-insensitivity of the CO oxidation on rhodium, its negative sensitivity on palladium and its positive sensitivity on platinum could be explained on the basis of 'single crystal data' gave impetus to the studies of the behaviour of nanoparticles in other catalytic systems.[82, 92, 93] For example, the results of TPD studies of NO molecules [92] provided an explanation for the 45-fold decrease in the rate of the CO + NO reaction with a decrease in the size of rhodium particles on $Rh/\alpha$-$Al_2O_3$ from ~ 70 to 1 nm (see Ref. 82). According to these data, the major part of the nitrogen

is desorbed from large particles at 463 K and only a small part is desorbed at 553 K. The amount of nitrogen adsorbed at high temperatures increases with decrease in the particle size. Stronger adsorption of nitrogen on the surface of small rhodium particles can be responsible for the structure-sensitivity of the CO + NO reaction on rhodium.[82] It is of note that the nature of the support ($\alpha$-$Al_2O_3$, $\theta$-$Al_2O_3$, $SiO_2$) has practically no effect on the activity of rhodium particles in this reaction.

Yet another example is the $CH_4 + O_2$ reaction and $O_2$ adsorption on $Pt/Al_2O_3$ catalysts with average sizes of platinum particles of < 2 and 20 nm.[94] It was found that the catalysts with larger particle sizes are ninefold more active in the methane oxidation, these are characterised by lower heats of oxygen adsorption (250 kJ $mol^{-1}$ instead of 280 kJ $mol^{-1}$ for smaller particles) and the oxygen adsorbed on them is more reactive with respect to hydrogen. The latter assumption is based on the fact that the oxygen adsorbed on a platinum catalyst with a particle size of 20 nm is totally desorbed by hydrogen at 195 K, whereas in the case of smaller platinum particles it does not react with hydrogen at temperatures up to 276 K. These findings point to a weakening of the bond between the platinum surface and the adsorbed oxygen with an increase in the particle size and a concomitant increase in the reaction rate.[94]

Studies aimed at establishing a relationship between the changes in the reactivities of nanoparticles and their electronic and structural properties are of fundamental importance.

The discovery of a dependence of the heat of desorption of CO on the crystallographic orientation of platinum faces[95–97] aroused debates concerning the effect of the structural factor on the heat of CO adsorption with changes in the particle size.[94] It is known that the spectra of the temperature-programmed desorption of carbon monoxide from the closely packed (111) face of platinum have the main peak at 400 K,[95] whereas its desorption from the more open (110) face of platinum or from platinum foil is accompanied by the appearance of an additional peak at 510 K, the relative intensity of the high-temperature peak being increased with an increase in the densities of the monoatomic steps.[96,97]

Comparison of spectra of temperature-programmed desorption of CO molecules from platinum single crystals and $Pt/Al_2O_3$ particles revealed that the weakening of the CO–Pt bond on large particles is due to predominant localisation on their surface of terraces the structure of which is identical with that of the (111) face, whereas small particles contain a large number of coordinatively unsaturated sites, which favours strengthening of this bond.[89] The presence of such low-coordinated sites was related to possible dissociation of the CO molecules on small platinum particles.[87] Their structure was simulated as a (100) step separating the (111) terraces. It was suggested that the repulsion of carbon atoms adsorbed on such sites from the CO molecules adsorbed on the (111) face of platinum weakens the CO–metal bond.[89]

The expediency of the structural approach is also confirmed by the fact that the shape of TPD spectra of the CO molecules did not depend on the orientation of the faces of Rh single crystals,[98,99] which is in complete agreement with the structure-insensitivity of the $CO + O_2$ reaction on rhodium-containing catalysts. The decrease in the heat of adsorption of oxygen and the corresponding increase in its reactivity with an increase in the size of platinum nanoparticles supported on alumina was attributed to the increased number of smooth areas on the catalyst's surface.

The electronic approach to rationalise unusual reactivities of metallic clusters was largely developed in studies with the use of methods suitable for the analysis of the nature of adsorbed particles together with the electronic properties of metal atoms.[10,100–103] Studies of CO adsorption on palladium, copper and nickel clusters supported on graphite revealed that a 'metal–dielectric' transition and strengthening of the CO–M bond with a decrease in the cluster size are observed within the same range of particle sizes.[103] It was found that in small particles the decrease in the intensity of the C 1*s* signal which is associated with the adsorbed CO ($E_b$ = 285.9 eV) occurs at higher temperatures. Moreover, the strengthening of the CO–M bond on nickel particles results in the dissociation of CO as can be evidenced from the appearance, in the TPD spectrum, of a C 1*s* signal with $E_b$ = 284.2 eV characteristic of elemental carbon, after heating of the sample to 300 K. It was assumed that the observed increase in the reactivities of small nickel particles with respect to the CO oxidation is accounted for by closeness of the 3*d*-levels of Ni and the $2\pi^*$-orbital of CO.

If the sizes of palladium and nickel nanoparticles are less than 3 nm, their metallic properties are weakened, which correlates with an increase in their reactivities towards oxygen[101] and hydrogen sulfide,[102] respectively. The conclusion about the strengthening of the O–Pd bond was based on data from microcalorimetry according to which the heat of adsorption of $O_2$ remains unchanged ($Q \approx 210$ kJ $mol^{-1}$) for particle sizes ranging from 1000 to 3 nm, but increases drastically (up to 335 kJ $mol^{-1}$) for smaller particles.[101] The nature of the support does not influence the heat of adsorption of $O_2$ on palladium particles sprayed over $SiO_2$, $\eta$-$Al_2O_3$ and $SiO_2$–$Al_2O_3$. The conclusion about enhanced dissociation of $H_2S$ on smaller nickel clusters is based on the increase in the relative intensity of the S 2*p* line ($E_b$ = 162.0 eV) characteristic of $S^{2-}$ ions in comparison with the line ($E_b$ = 164.5 eV) related to hydrogen sulfide adsorbed as a molecule with a decrease in the particle size.[102]

One should not rule out the possibility that the proportion of rough surfaces in particles with sizes varying from 3 to 5 nm is greater, since they contain a large number of low-coordinated atoms on the steps, in the edges, *etc*. Apparently, the electronic and structural factors are closely interrelated and their effects on the reactivities of metallic clusters cannot be differentiated. The correctness of this statement can be illustrated by the results of experiments carried out by Zilm *et al*.[10] Comparison of $^{13}C$ NMR spectra of adsorbed CO molecules recorded with and without magic angle spinning allowed the authors to suggest that the significant decrease in the diffusion rates of carbon monoxide on the surface of small palladium particles is due to stronger binding of CO to these particles. It was concluded that strongly bound CO with a lowered ability for diffusion is linearly adsorbed on edge and corner palladium atoms the proportion of which increases with a decrease in the particle size. Moreover, comparison of the Knight shift for the linear and bridge-like forms of CO demonstrated that these low-coordinated sites are characterised by electron deficiency resulting from changes in their Fermi levels relative to those of the bulk metal.

It is worth noting that the differences in the properties of the conductivity electrons of supported nickel[30] and silver[31,32] particles, on the one hand, and those of the corresponding bulk metals, on the other hand, also correlate with changes in the surface structures of the particles, which become more defective after their treatment with the reaction medium. In the case of Ni–C catalysts for butadiene hydrogenation, this conclusion was based on TEM data, whereas for silver particles active in ethylene epoxidation it was based on the disappearance, from the XPS spectra, of the O 1*s* line characteristic of the adsorbed oxygen.

The variations in the routes of NO decomposition and the CO + NO reaction with a decrease in the size of palladium particles supported on silica was explained by the effect of low-coordinated sites, with lower electron density on the NO adsorption.[103] The strengthening of the NO–Pd bond in such low-coordinated sites the existence of which was confirmed by comparison of infrared absorption spectra of CO molecules adsorbed on palladium particles and on (111) and (110) faces of palladium single crystals,[104,105] favours the dissociation of NO into nitrogen and oxygen atoms. In the absence of NO adsorbed as molecules on the surface of small palladium particles, $N_2O$ cannot be formed as was demonstrated using the temperature-programmed reaction (TPR).

As mentioned above, the number of papers which attribute the changes in selectivity caused by a decrease in the size of metallic

nanoparticles to changes in the chemical nature of their surface adsorption in comparison with adsorption on bulk metals will unquestionably be increasing. The above-cited NMR studies of CO adsorption on palladium supported on $SiO_2$ represent a first step in this direction.[10] It was shown that two types of CO molecules on the surfaces of small palladium particles differ in the degree of mixing of their electronic levels with the electronic zones of the metal.

The correlation between the nature of the adsorbed molecules and the catalytic properties (in the first place, selectivities) of supported nickel and silver particles has been demonstrated.[30, 31, 106] The TPD spectra of hydrogen following its adsorption for 2 min on two catalysts of selective hydrogenation of butadiene differing in their Ni : C ratios are depicted in Fig. 3. The selectivity of butadiene hydrogenation to butene on a catalyst with a low carbon content (Ni : C ratio of 0.4) was 45%, whereas that on a catalyst with a higher carbon content (Ni : C ratio of 0.1) reached 95%.[30] As can be seen from Fig. 3, the more selective catalyst gives one TPD peak at 320 K, whereas the TPD spectrum of the less selective specimen contains a weakly expressed additional peak corresponding to more strongly bound hydrogen (at 360 K). These peaks were assigned based on the TPD data and work function measurements of hydrogen adsorption on specimens of bulk nickel (single crystals and foil) obtained in earlier studies.[107, 108] In experiments where hydrogen exposure varied, it was established that hydrogen in a high-temperature form is initially adsorbed on the nickel surface and the work function increases markedly. The TPD peak at 360 K was ascribed to the negatively charged hydrogen ions, $H^-$. The intensity of the high-temperature peak becomes constant with an increase in the hydrogen exposure, whereas the 320 K peak continues to increase gradually. The work function did not change in the studied range of coverage of the nickel surface with hydrogen, which points to the absence of a charge on the low-temperature form of hydrogen.[107] High reactivity of hydride ions is a possible reason for non-selective hydrogenation of butadiene on specimens with high Ni : C ratios ($\sim 0.4$). The lack of this form in specimens with the Ni : C ratio of $\approx 0.1$ (see Fig. 3) is the reason for increased selectivity. Unfortunately, these conclusions cannot be corroborated by XPS, since hydrogen does not generate a photoelectron spectrum.

This approach is quite useful in studies of different forms of oxygen adsorption on silver. The screening of O 1*s* signals from the adsorbed oxygen by the oxygen of the substrate ($\alpha$-$Al_2O_3$) used in industrial catalysts of ethylene epoxidation was eliminated by replacing the latter with a model substrate (graphite).[106] The oxygen adsorbed on the surface of silver particles with the sizes of 10 nm produces one peak with $E_b = 530.5$ eV, while larger particles produce an additional peak with $E_b = 528.5$ eV. Comparison of these values with the $E_b$ values for oxygen adsorbed on bulk silver specimens prompted a conclusion about the formation

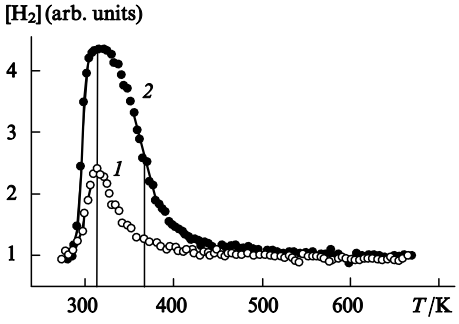



**Figure 3.** The TPD spectra of hydrogen after its 2-min adsorption at $P = 10$ Pa and $T = 270$ K on Ni–C catalysts with the Ni : C ratio of 0.1 (*1*) and 0.4 (*2*).

of two forms of oxygen adsorbed as atoms, *viz*., the peak with a lower binding energy is related to nucleophilic oxygen ($O^{2-}$), while the second peak is related to the electrophilic form ($O^{\delta-}$). It was shown [109, 110] that the formation of ethylene oxide requires the co-existence of these two forms of the adsorbed oxygen on the silver surface: the electrophilic oxygen participates in the formation of ethylene oxide directly by reacting with ethylene, while the nucleophilic oxygen serves as a source of surface $Ag^+$ ions (surface silver oxide), which are the sites of adsorption of ethylene molecules. The key step of the ethylene epoxidation can be presented as follows:

$$O^{\delta-}_{ads} + C_2H_{4\,ads}(Ag^+) \longrightarrow C_2H_4O.$$

With account taken of the sharp drop in the concentration of nucleophilic oxygen with a decrease in the size of the silver particles in the range of 50–20 nm, the mechanism proposed provides an explanation for the sharp decrease in the rate of epoxidation on silver catalysts with a particle size of less than 50 nm.[76] The reaction rate decreases as a result of less effective adsorption of ethylene on small particles which contain no $Ag^+$ sites. Since the nucleophilic oxygen is active exclusively in complete oxidation of ethylene, its disappearance due to a decrease in the size of the catalyst's nanoparticles will increase the selectivity of ethylene oxide formation. This suggestion has been confirmed experimentally by Verykios *et al.*[111] who have observed a continuous increase in the selectivity with a decrease in the size of silver particles from 50 to 20 nm. These data and the results of other investigations [109, 110] suggest that this size range is an optimum for particles of highly reactive and highly selective silver catalysts for ethylene epoxidation.

Studies of the dependence of selectivities of chemical reactions on the average sizes of coated nanoparticles of the active components revealed both positive and negative effects and, in some cases, their independence of the particle size (see, *e.g.*, Refs 112–114). We shall consider only the results of several experiments which are promising for use in practical catalysis.

The dependence of selectivities of the synthesis of higher hydrocarbons from CO and $H_2$ on Co–MgO and Co–ZnO catalysts on the sizes of coated cobalt particles was established.[115] The smaller the average sizes of cobalt nanoparticles, the higher the selectivity expressed by the Anderson–Schulz–Flory distribution coefficient ($\alpha$). It was suggested that the amount of dissolved hydrogen responsible for complete hydrogenation of hydrocarbon intermediates decreases with a decrease in the particle size, eventually resulting in the formation of heavier hydrocarbons. The selectivity of hydrodesulfurisation of thiophene increased with a decrease in the sizes of ruthenium nanoparticles supported on alumina.[116] Comparison of $Co/Al_2O_3$ catalysts accelerating steam conversion of ethanol and prepared from different Co-containing precursors revealed that the selectivity of this reaction decreases in the following order: Co (carbonyl) > Co (chloride) > Co (acetate) > Co (nitrate).[117] Since the sizes of metal particles increase in the reverse order, the observed decrease in selectivity was attributed to the enlargement of cobalt nanoparticles. And, finally, it was found [118] that the selectivity of n-pentane hydrogenolysis on Pt/Y-zeolite catalysts increases linearly with decrease in the size of the metallic nanoparticles.

Even these few examples illustrate the remarkable effects of the average sizes of active metal nanoparticles on the relative rates of individual steps of multiroute catalytic reactions which influences the selectivities of formation of the reaction products. The catalytic activities manifested by nanosystems in reactions in which bulk specimens or even supported large crystallites are virtually inactive corroborate this statement. Gold nanoparticles which, in contrast with the bulk metal, manifest catalytic activity in certain reactions including those promising for industrial use, provide an illustrative example. In the 1980's, Japanese investigators succeeded in demonstrating that Au nanoparticles supported on $Fe_2O_3$ or $Co_3O_4$ represent active catalysts for low-temperature oxidation of CO.[119] This finding has stimulated the

appearance of numerous publications devoted to the analysis of the catalytic properties of these systems. The dependence of their catalytic properties on the nature of the substrate, size of gold particles and further treatment of freshly prepared specimens was studied.[120–125] It was shown that the size of gold nanoparticles is the key factor which determines the activity of a catalyst in CO oxidation; this activity changes 2–3-fold with different substrates ($TiO_2$, $Al_2O_3$, $SiO_2$), whereas the reaction rate increased by one and even two orders of magnitude with a decrease in the gold particle sizes below 4 nm.[120–122] The maximum catalytic activity was observed in particles with a size of 3.2 nm.[123] It is of note that gold-containing catalysts manifest high activity even at low temperatures (250–270 K), whereas such a catalytically active metal as platinum is inactive at these temperatures due to the blocking of its surface by adsorbed CO molecules.[126]

The range of reactions catalysed by gold nanoparticles appeared to be rather broad. It was demonstrated that impregnated $Au/SiO_2$ and $Au/Al_2O_3$ catalysts manifest high selectivities in the hydrogenation of buta-1,3-diene to butene.[127] The selectivity of hydrogenation of diene mixtures into alkenes on $Au/ZrO_2$ catalysts reached 100%.[128] Studies into hydrogenation of $CO_2$ on Cu-, Ag- and Au-containing catalysts supported on $ZrO_2$ revealed that these metals are catalytically active in methanol synthesis.[129] Gold nanoparticles used as catalysts for low-temperature reduction of NO with propene have certain advantages.[130] Unlike Rh-,[131] Pt-[132] and Pd-containing[133] catalysts with which $N_2$ is formed instead of $N_2O$ at temperatures above 570 K, the formation of nitrogen on $Au/Al_2O_3$ proceeds efficiently even at 370 K.

The use of gold nanoparticles as catalysts of propene epoxidation provides a more interesting example. The gas-phase oxidation of propene by an oxygen–hydrogen mixture on $Au/TiO_2$ catalysts ensures nearly 100% selectivity of propene oxide formation at a 1% conversion of $C_3H_6$.[134] A detailed study of various factors revealed that the selectivity of this reaction depends critically both on the nature of the substrate and the size of gold nanoparticles. If the particle size is less than 2 nm, the reaction performed on gold catalysts changes its route in such a way that propane is formed with nearly 100% selectivity.[135] This finding is in good agreement with the high activity of the low-percentage $Au/SiO_2$ catalyst in the hydrogenation of alkenes.[136] It may thus be concluded that gold nanoparticles with sizes ranging from 2 to 4 nm catalyse propene epoxidation, whereas smaller particles catalyse its hydrogenation. It was found that the selectivity of formation of some industrially important products increases considerably with a decrease in the particle size.[137,138] For example, $Pt_n$ clusters within the structure of the zeolite LTL provided a nearly 100% selectivity of dehydrogenation of n-hexane to benzene.[137]

A vast variety of physical instrumental methods, such as molecular beam technique, low energy electron diffraction, electronic Auger spectroscopy, photoelectron X-ray spectroscopy, vacuum tunnelling microscopy, nuclear magnetic resonance, electron spin resonance, Raman spectroscopy, calorimetry, TPR, TPD, infrared spectroscopy, EXAFS, Mössbauer spectroscopy, *etc*., came into use in the last decades of the XXth century for studying surfaces of heterogeneous catalysts at the molecular level. However, despite the high precision achieved in the techniques for measuring and the control of the state of the catalytic surfaces, the 'cognitive' potential of the experimental results is rather limited because these measurements are usually indirect and the information derived from them demands quantitative processing and interpretation. This can be done only with the use of mathematical models. It is clear that successful interpretation of the results obtained requires that the mathematical models and the methods employed for their analysis provide an accurate description of the whole body of experimental results.[139–146]

The lattice gas model is an example. The main difference between ordinary and lattice gases is that in the former case a particle can have any coordinates, whereas molecules of lattice gases occupy definite positions in space, *viz*., those in the knots of a certain regular lattice where elementary processes can occur. These processes are described either by computational methods conventionally used in statistical physics (*e.g*., the Monte-Carlo and cellular automaton methods) or by using cluster approximations, which allow simple estimation of thermodynamic parameters of a system and the rates of elementary surface acts based on the classical transition state theory developed by M I Temkin for heterogeneous catalysis.

Sequential implementation of a series of elementary steps results in changes in the state of the lattice cells and the evolution of the system. The Monte-Carlo method considers evolution as a random Markovian chain of elementary events occurring in the lattice cells. The cellular automaton approach also represents an effective tool for simulating the dynamics of elaborate spatially distributed systems based on the analysis of their local behaviour. To obvious disadvantages of stochastic methods, one can relate the large body of calculations, whereas their main advantage is the possibility of precise control over the position of a particle on the surface of a catalyst. The deterministic approach entails the solution of systems of nonlinear differential equations derived from the main kinetic equation using certain approximations.

The energy of lateral interactions of the adsorbed species involved in reactions and their mobilities are the main parameters which characterise their surface layer. The latter represents an open, non-ideal, non-linear system which exchanges mass and energy with the environment. The use of the non-linear dynamics method made it possible to gain considerable experience in mathematical simulation of catalytic systems starting at the molecular level.[143–146] Non-linear events, such as self-organisation, the appearance of chemical turbulence, *etc*., have also been studied. However, the attempts to simulate the effects of the particle size on such events have not been undertaken yet.

## IV. The prospects for the application of nanostructures in catalytic processes

### 1. Ligand-stabilised transition metal clusters

The catalytic properties of supported particles can differ essentially from those of bulk metals; therefore, new routes of catalytic processes should not be ruled out. It can thus be assumed that the advantages of nanostructures prepared by conventional methods as highly selective catalysts cannot always be realised due to the broad size distribution of particles and their sintering in the course of the catalyst's operation. In supported metallic catalysts obtained by industrial synthesis, which includes impregnation of substrate granules with solutions of active metal compounds followed by calcination and/or reduction, strong interactions between metallic nanoparticles and the substrate surface are usually absent, which results in the statistical distribution of particles according to their sizes and also facilitates their sintering.

There are several ways to solve this problem, namely, modification of the support aimed at generating a sufficient number of centres for nucleation of metallic particles,[147] the choice of materials (a substrate and an active component) providing the epitaxial growth of nanoparticles owing to the structural matching of parameters of crystal lattices,[148] the use of novel substrates with an original geometry of the pore volume,[149] *etc*. The size homogeneity of nanostructures can be achieved through the use of ligand-stabilised metallic clusters.[150,151] Isolated transition metal nanoclusters which are the most commonly used as active components of supported metal catalysts, are prepared by the following techniques: (1) reduction of transition metal salts; (2) reduction and removal of ligands from organometallic compounds; (3) electrochemical synthesis.[151] Studies into the kinetics of growth of nanoclusters revealed that clusters containing the so-called magic number of atoms are characterised by regular geometry of the outer surface and manifest enhanced stabilities. The other name of these clusters, *viz*., 'full-shell clusters', reflects the presence of fully packed layers surrounding the central metal atom. The number of

the metal atoms ($N$) in the $n$th-layer is determined by the equation:[151]

$$N = 10n^2 + 2 \ (n > 0). \quad (3)$$

Thus, full-shell clusters contain 13 (1 + 12); 55 (13 + 42); 147 (55 + 92); 309 (147 + 162), *etc*., atoms (see Section II.I). The enhanced stabilities of these clusters stem from their closely packed structures which ensure the formation of the maximum number of metal–metal bonds and, as a consequence, the minimum surface energy.

An excellent survey of growth mechanisms of nanoclusters has been given in reviews.[152–154] It was shown that the formation of iridium nanoclusters stabilised by the $P_2W_{15}Nb_3O_{62}^{9-}$ polyoxoanion follows an autocatalytic surface growth mechanism, which provides an explanation for the formation of isolated full-shell clusters in a kinetically controlled regime of synthesis. Experimental evidence for these conclusions can be derived from the formation of nearly monodisperse rhodium nanoclusters ($d = 4\pm0.6$ nm) in the reduction of polyoxoanionic Rh(I) complexes with hydrogen in acetone.[154]

The nature of nanoclusters stabilised by ligands entails the possibility of their additional stabilisation by electrostatic and steric interactions. Electrostatic or inorganic stabilisation is achieved by adsorption of ions on the electrophilic surface of a metal.[155] Such adsorption results in the appearance, on the surface of nanoclusters, of a double electrical layer which provides Coulombic repulsion of like-charged individual species. Steric or organic stabilisation is provided by the surrounding of the metal centre of the nanocluster with a layer of bulky structures,[155] such as polymeric units[156] or surfactants.[157] The geometric sizes of these adsorbates favour the formation of a steric barrier which prevents the contacts between the metal centres of nanoclusters. It is evident that some of the stabilising agents, *e.g*., polyoxoanions, combine electrostatic and steric functions.[151, 158] Stabilisation of nanoclusters with ligands presents substantial interest as regards the synthesis of supported catalysts characterised by enhanced stabilities and homogeneous size distribution of metal particles. In addition, this makes the use of metallic nanoclusters promising for homogeneous catalysis, as will be shown below.

The catalytic properties of metallic nanoclusters have been studied by several groups of investigators (for a review see Ref. 151). In 1981, Schmid *et al*.[159] succeeded in synthesising a cluster with the composition $Au_{55}(PPh_3)_{12}Cl_6$ by passing $B_2H_6$ through a solution of $PPh_3AuCl$ in benzene. Later, $Rh_{55}(PPh_3)_{12}Cl_6$, $Ru_{55}(PBu^t_3)_{12}Cl_{20}$, $Pt_{55}(AsBu^t_3)_{12}Cl_{20}$ clusters were synthesised using diborane as the reductant.[160, 161] Substitution of hydrogen for diborane made possible the synthesis of $Pt_{\sim309}phen_{\sim36}O_{\sim30\pm10}$ and $Pt_{\sim561}phen_{\sim36}O_{\sim190-200}$ clusters.[162, 163] As can be seen, all these clusters are 'magic' ones, which provides additional evidence in favour of enhanced stabilities of the full-shell nanostructures cited above. First attempts at using Ru clusters as catalysts in homogeneous hydrogenation reactions were unsuccessful because of their rapid decomposition.[163] Therefore, further efforts of this research group were directed to the use of nanoclusters for the synthesis of supported heterogeneous catalysts. It was shown that palladium clusters with sizes of 3–4 nm stabilised by ligands manifest high activities and selectivities in the hydrogenation of hex-2-yne into *cis*-hex-2-ene. It was shown that the activity of a catalytic system depends on the nature of the stabilising ligands, while the selectivity is always equal to 100%. Rhodium and palladium nanoclusters supported on $TiO_2$ and $Al_2O_3$ appeared to be highly efficient catalysts of hydroformylation[164] and hydrogenation[165] reactions.

Unlike the authors of the above-cited papers, in the early 1980's Vargaftik, Moiseev *et al*.[166] carried out a successful synthesis of ligand-stabilised clusters which are active and stable in homogeneous catalysis. The $Pd_{\sim561}phen_{\sim60}(OAc)_{\sim180}$ and $Pd_{\sim561}phen_{\sim60}O_{\sim60}(PF_6)_{\sim60}$ clusters catalysed oxidative acetoxylation of a series of light organic compounds, *e.g*., of ethylene into vinyl acetate, of propene into allyl acetate and of toluene into benzyl acetate, with 95%–98% selectivity. Moreover, these catalysts effected the oxidation of primary alcohols into ethers and aldehydes and of secondary alcohols into ketones.[166] Yet another example of a successful application of metallic nanoclusters in homogeneous catalysis is the use of rhodium clusters stabilised by polyoxoanions, which manifested high selectivities in the hydrogenation of cyclohexene.[154] This was ascribed to the double stabilisation (both electrostatic and steric) of the clusters by polyoxoanions.[167]

Notwithstanding, the majority of successful applications of metallic nanoclusters as catalysts is connected with the use of systems fixed or immobilised on the surface of porous and non-porous supports, *e.g*., $SiO_2$, $Al_2O_3$ or $TiO_2$. It was shown, in particular, that 5% colloidal rhodium supported on activated charcoal with a narrow size distribution of clusters (1.2–2.2 nm) was nearly 3 times more active in the hydrogenation of butyronitrile than the corresponding industrial catalyst which also contains 5% Rh on activated charcoal with a greater scatter of particle sizes (1–5 nm).[168] In catalysts stabilised by ligands, the size of rhodium particles varies from 1.2 to 2.0 nm, whereas standard catalysts contain predominantly large crystallites, while the fraction of small particles (1–5 nm) is small. A representative list of reactions which are efficiently catalysed by clusters stabilised by ligands is given in a review.[151] This list includes various reactions of enantioselective hydrogenation,[169] hydrosilylation,[170] hydropyrolysis and hydrogenolysis,[171] CO and CO + $H_2$ oxidation,[172] cycloaddition reactions,[173] *etc*.

This can be supplemented with examples of enhanced stabilities of catalysts based on clusters stabilised by ligands under conditions of a catalytic reaction. Thus the 'lifetime' of a catalyst containing palladium nanoclusters in the reaction of cyclooctene hydrogenation was 96 000 turnovers, whereas that of an industrial catalyst (*e.g*., palladium on activated charcoal) was 38 000 turnovers.[168] The $Ir_{\sim300}$ nanoclusters did not change their activities after $3200\pm1000$ hydrogenation turnovers, which is comparable with the corresponding value ($3950\pm1000$ turnovers) for the industrial catalyst (7.9% $Ir/\gamma$-$Al_2O_3$) and markedly exceeds the 'lifetime' of $Ir/\eta$-$Al_2O_3$ ('Exxon', USA) equal to $1740\pm250$ turnovers.

Ligand-stabilised metallic clusters are extremely interesting subjects for the development of fundamental concepts of catalysis by nanostructures, since it allows one to control precisely the size distribution of nanoparticles, to establish relationships between their sizes and catalytic properties and even to govern the activities and selectivities of catalysts based on them. However, the high cost of such catalysts in comparison with ordinary specimens is an obstacle to their wide industrial application. Only electrochemical synthesis makes it possible to prepare relatively large (*e.g*., hundreds of milligrams) amounts of catalysts based on metal clusters stabilised by ligands. Therefore, industrial applications of such nanoclusters in large-scale catalytic processes is hardly probable. However, their use in fine organic syntheses where high selectivity of formation of the target product is the main requirement imposed on a catalyst can be of considerable practical interest. It is anticipated that the attainment of 100% selectivity will become one of the main challenges to catalytic science in the next few decades.[174] This can be exemplified by successful recent applications of clusters stabilised by ligands in various hydrogenation reactions including enantioselective hydrogenation.[175, 176]

## 2. Bimetallic clusters: molecular design of active centres

Studies into bimetallic systems have the same long history as studies of individual metals. This is primarily due to the search for the ways of increasing the activities, selectivities and stabilities of monometallic catalysts. The first patents which suggested the use of Pd–Au catalysts for hydrocarbon conversions instead of palladium ones appeared in the 1960's.[177] In the past years, the number of investigations (including those having industrial applications) which demonstrate the advantages of bimetallic catalysts

over monometallic ones has increased manifold.[178–184] Most of these studies dealt with the dependences of catalytic activities related to the surface metal atoms and their selectivities on the ratios of metals. For example, the maximum activity of Pt–Re/$SiO_2$ catalysts containing 75% rhenium exceeds those of individual platinum and rhenium supported on $SiO_2$ by more than two orders of magnitude.[180] Rubidium, palladium or platinum additives increased the activities of nickel-containing zeolites in butyronitrile hydrogenation in both gas and liquid phases.[181] The steady-state activity of Pd–Re/$Al_2O_3$ catalysts in the hydrogenolysis of 2,2-dimethylpropane passes through an obvious maximum at a rhenium content of 50 at.%.[182] Examples of enhanced selectivity in the formation of various products through multiroute catalytic reactions are even more impressive. The above-cited patent[177] claims that the selectivity of n-heptane isomerisation increases from 66.9% to 81.3% with a change in the Pd : Au ratio of Pd–Au/$Al_2O_3$ catalysts from 6 : 1 to 1 : 2 (mass %). The selectivity of monometallic palladium and gold catalysts is equal to 50% and ~ 25%, respectively. The selectivity of 1% Ru/$SiO_2$, which is a catalyst of cyclohexane dehydrogenation to benzene, increases, following introduction of inactive copper and silver (1 mass %), from 76% to 94% and 87.9%, respectively.[183] The enhanced selectivity of nitrogen formation and decreased yields of ammonia were observed in the reduction of NO with hydrogen with an increase in the rhenium content in bimetallic Pt–Re/$SiO_2$ catalysts.[184] Modification of platinum nanoparticles on silica with tungsten made it possible to reach 99.2% selectivity of methanol formation in the reaction of $CO_2$ with hydrogen, the conversion being 2.6%.[185] It is of note that platinum alone catalyses the formation of CO with nearly 100% selectivity, whereas tungsten is inactive in this reaction. It was shown[181] that all M–Cu/NaY catalysts (M = Ru, Rh, Pd, Pt) manifest high selectivities in the formation of tertiary amines from acetonitrile.

The unusual properties of bimetallic catalysts gave impetus to the studies of their surface using model systems and sensitive physical methods. The experimental results have been generalised in the reviews.[186, 187] It was found that the introduction of a second metal influences the catalytic properties of the first metal through the following mechanisms:

(1) by changing the electronic properties of the first metal atoms (as has been shown previously, the electronic properties of metals influence the nature and reactivities of adsorbed particles);

(2) by changing the number of identical atoms within the structure of the adsorption centre (as is known, adsorption of molecules from the gas phase often requires a combination of specifically arranged atoms rather than a single 'landing' site).

In the first case, we deal with an electronic (ligand-associated) effect, whereas in the second case the multiplet ensemble effect is manifested.[178, 186, 187] With regard to real catalysts, this is, most probably, artificial, therefore, the existence of such effects has been demonstrated using only model systems.

Direct evidence for the electronic effect was obtained in experiments with adsorption of simple gases on the surface of a metal single crystal covered with a monolayer of atoms of another metal. Concrete systems for such experiments were selected on the basis of structural matching of this monolayer and the plane of a metal substrate.[188–191] For example, a palladium monolayer was deposited onto the (110) face of tungsten the hexagonal structure of which ensured a practically complete coincidence of Pd–Pd distances in the monolayer (0.2740 nm) and onto the (111) face of the bulk Pd single crystal (0.2751 nm).[188] The activation energy of desorption of CO molecules from the surface of Pd/W(110) appeared to be by 85 kJ $mol^{-1}$ smaller than that from the surface of the Pd(111) single crystal. In addition, the preexponential factor in the equation of CO desorption rate increased by five orders of magnitude. Combined use of both factors caused a decrease in the desorption temperature from 510 K on Pd(111) to 330 K on the monolayer of Pd/W(110) in the case of a low degree of coverage by CO. A similar effect was observed when palladium was deposited onto the surface of the Re(0001) hexagonal face.[189] An analysis of UV photoelectron spectra of the palladium monolayer on the (110) faces of tantalum[190] or niobium[191] revealed that the densities of filled electronic states of palladium near the Fermi levels in these systems are significantly decreased in comparison with that on Pd(111). As a result, the electronic structure of the surface layer of palladium becomes similar to that of the Group IA metals characterised by weak chemosorption bonds with CO. This can be explained by the formation of covalent bonds between palladium and niobium due to rehybridisation of *d*- and *sp*-orbitals, although a small charge transfer can also take place. Alloys with high negative enthalpies of formation are related to the systems in which the electronic effect plays a crucial role.[187]

Depending on the strength of the interaction between the main and incorporated metals, the ensemble effects are conventionally divided into simple and mixed ones.[186, 187] Simple effects are largely manifested in systems where a reactive metal is mixed with an inert one. For example, the multibound state of CO on platinum and nickel is not realised following their fusion with copper.[192, 193] The triply bound form of NO which predominates on the (111) face of platinum is not detected on the surface of the $(3 \times 3)$-$SnPt_2$/Pt(111) alloy where triatomic platinum multiplets are completely absent.[194] Decisive evidence for the existence of a mixed ensemble effect was obtained in the study of a copper monolayer deposited onto the (111) face of nickel single crystals.[195, 196] Despite the higher strength of binding of the bridge-like form of CO to the nickel surface in comparison with the linear form, the latter was exclusively formed at low coverage of carbon monoxide. This was inferred from the results of high-resolution electron energy loss spectroscopy (HREELS) which point to the absence of Ni—Ni couples on the surface of this bimetallic system. However, a bridge-like form was also detected at higher degrees of CO coating, which is due to the presence of Ni—Cu couples.[196]

The mutual effects of individual components are characteristic of many bimetallic systems. Therefore, several attempts have been undertaken to use these regularities for the directed synthesis of bimetallic catalysts with predetermined properties. Thus Besenbacher *et al.*[197] proposed to introduce atoms of gold into a nickel-containing catalyst of the steam conversion of methane in order to reduce the rate of its coking. The choice of gold was based on the results of fundamental investigations of single crystals and porous specimens of the catalyst using physical methods and quantum-chemical calculations of activation energies of the abstraction of the first hydrogen atom from the methane molecule and carbon atom adsorption on pure and modified nickel surfaces. The conditions for gold introduction were also established. This resulted in the synthesis of an Au—Ni bimetallic catalyst, which, in contrast to the nickel catalyst, preserved its activity in n-butane conversion due to the absence of graphite deposits on its surface.

The most remarkable achievements in the design of bimetallic catalysts can be expected from the use of nanoclusters which allows molecular design of active centres. There exist several synthetic routes which ensure control over the composition and properties of the nanostructures formed,[198] *viz.*, combined or sequential reduction of metal salts, electrochemical synthesis and reduction of double complexes. Studies of synthetic nanoclusters by physical methods aimed at elucidating their structures acquires special importance, since in addition to the crystal structure of the bulk alloy, bimetallic nanoclusters contain unusual structures which have no analogues among bulk materials. These include two types of structures, *viz.*, 'core–shell' and 'cluster-in-cluster' types.

Core–shell structures were detected in Pd—Pt clusters stabilised by poly(*N*-vinyl-2-pyrrolidone) (PVP) with a Pd : Pt ratio of 4 : 1; they were prepared by the reduction of a $H_2PtCl_6$—$PdCl_2$ mixture.[199–201] Elucidation of exact structures of these nanoclusters required the use of a combination of methods, *e.g.*, X-ray phase analysis, TEM, XPS, UV-visible absorption spectroscopy (UV-Vis) and EXAFS. Analysis of the UV-Vis spectra and X-ray diffractograms confirmed the formation of bimetallic nanoclus-

ters. Using the TEM approach, it was shown that the Pd–Pt clusters formed are homogenous according to their sizes (the mean size was 1.5 nm) and belong to 'magic' clusters with $N = 55$.[169] A conclusion about the saturation of the nanocluster surface with palladium was inferred from the quantitative XPS data.[202] And, finally, the coordination numbers for palladium and platinum were determined using EXAFS. Comparison of experimental results with the values calculated for two models, *viz*., a model with inner platinum nuclei and a statistical distribution model, revealed that the former best fits the experimental results.[199] The experimental data altogether allowed one to propose a structural model of a Pd–Pt nanocluster in which a monolayer of 42 palladium atoms covers a nucleus consisting of 13 platinum atoms.[198] Later, bimetallic nanoclusters containing core–shell structures could successfully be obtained by stabilisation of Pd–Au, Pt–Au and Rh–Pt systems by polyvinylpyrrolidone.[203, 204]

In bimetallic nanosystems of the 'cluster-in-cluster' type, the atoms of one component form a cluster, whereas the atoms of the other component cover only some of its planes (not necessarily as a monolayer) to form an intertwining structure. The fact that such structures are formed in Pd–Au clusters with a change in the Pd : Au ratio from 4 : 1 to 1 : 1,[203] implies that it can represent a modified structure with an inner nucleus. Additional evidence in favour of this suggestion can be derived from the transformation of Pd–Pt nanoclusters with inner nuclei into 'cluster-in-cluster' structures in their application onto inorganic materials.[205] Without going into details about the similarities and differences of these two structures, it should be noted that the surface of nanoclusters of the 'cluster-in-cluster' type contains some centres which consist of two kinds of atoms, *i.e*., the ensemble effect is possible, whereas only the electronic (ligand) effect is *a priori* possible in structures with inner nuclei.

It is the ligand effect that is responsible for the enhanced catalytic activities of PVP-stabilised Pd–Pt clusters in the hydrogenation of cycloocta-1,3-diene into cyclooctene. Indeed, the maximum increase in activity (more than twofold in comparison with pure palladium) was observed for the Pd : Pt ratio of 4 : 1,[200] *i.e*., under conditions where palladium atoms completely covered the inner platinum nucleus. A similar dependence was observed in the case of Pd–Au nanoclusters.[203] The fourfold increase in the catalyst's activity in comparison with those of individual components was observed in the hydrogenation of cyclopentadiene into cyclopentene on Pd–Rh nanoclusters.[198]

Yet another example of the ensemble effect is the reaction of selective hydration of acrylonitrile to acrylamide:

$$CH_2=CH-CN + H_2O \longrightarrow CH_2=CH-CONH_2$$

on bimetallic Cu–Pd nanoclusters stabilised by PVP.[206] It was found that this reaction occurs on two adjacent palladium and copper atoms: the coordination of the C=C bond takes place on the palladium atom, which brings the C≡N bond close to the adjacent copper atom which effects hydration. This results in the enhancement of activity and nearly 100% selectivity of the amide synthesis. It was shown also that the supported Pd–Mo/$SiO_2$ catalyst based on a bimetallic precursor manifests higher activity in the CO + NO + $O_2$ reaction than analogous specimens synthesised from individual organometallic complexes.[207]

## V. Conclusion

The fundamental knowledge of catalytic properties of nanosystems at the molecular level and practical application of their peculiarities largely determine progress in industrial catalysis and, correspondingly, the economic potential of certain branches of the chemical industry and the environmental situation.

The unique microstructures of nanosystems in comparison with ordinary metals and chemical compounds confer novel properties on them. The characteristic features of nano- and microgeometry of nanosystems and their high specific surfaces open up new opportunities for the design of highly selective and highly reactive perfect catalysts. Some of these features can be synergistic, *e.g*., in bimetallic clusters where one component influences the properties of the adjacent component. Detailed investigations into such interactions will allow the synthesis of novel selective catalysts with predetermined properties. It is the selectivity that is the key problem in the theory and practice of catalysis. And if the problems of sizes and compositions of nanoclusters which ensure their optimum selectivity, detailed electronic structures of cluster complexes, *etc*., are solved, surface reactivity will be put under control.

Nanosystems are a 'natural bridge' between homogeneous and heterogeneous catalysis. Many metals, especially Group VIII metals, which manifest the highest activity as heterogeneous catalysts form numerous cluster compounds endowed with unique catalytic properties. The chemistry of these elements has been studied in sufficiently great detail and the dependence of physicochemical properties of the corresponding clusters on their sizes has been established. However, in more general terms the state-of-the-art in the studies of catalytic activities of nanosystems can be characterised as 'abundance without order'. The main task for the next few years is to combine experimental studies aimed at the construction of new active catalysts based on nanosystems with theoretical (including quantum-mechanical) calculations and more extensive use of physical (both instrumental and diagnostic) methods as well as kinetic studies and mathematical simulation.

This review has been written with the financial support of the Russian Foundation for Basic Research (Project Nos 96-03-33891 and 00-15-99-335).

## References

1. W L Winterbottom *Acta Metall.* **15** 303 (1967)
2. T Wang, C Lee, L D Schmidt *Surf. Sci.* **163** 181 (1985)
3. M Drechsler *Surf. Sci.* **162** 755 (1985)
4. M Drechsler, J M Dominguez *Surf. Sci.* **217** L406 (1989)
5. K Hayek, M Fuchs, B Klotzer, W Reichl, G Rupprechter *Top. Catal.* **13** 55 (2000)
6. A Piednoir, E Perrot, S Granjeaud, A Humbert, C Chapon, C R Henry *Surf. Sci.* **391** 19 (1997)
7. X Lai, T P St Clair, M Valden, D W Goodman *Prog. Surf. Sci.* **59** 25 (1998)
8. K H Hansen, T Worren, S Stempel, E Lœgsgaard, M Bäumer, H-J Freund, F Besenbacher, I Stensgaard *Phys. Rev. Lett.* **83** 4120 (1999)
9. M Bäumer, H-J Freund *Prog. Surf. Sci.* **61** 127 (1999)
10. K W Zilm, L Bonneviot, G L Haller, O H Han, M Kermarec *J. Phys. Chem.* **94** 8495 (1990)
11. X Xu, J Szanyi, Q Xu, D W Goodman *Catal. Today* **21** 57 (1994)
12. D W Goodman *Surf. Sci.* **299**/**300** 837 (1994)
13. C Backx, C P M de Groot, P Biloen, W M H Sachtler *Surf. Sci.* **128** 81 (1981)
14. C T Campbell *Surf. Sci.* **143** 517 (1984)
15. C T Campbell *Surf. Sci.* **157** 43 (1985)
16. R Kubo *J. Phys. Soc. Jpn.* **17** 975 (1962)
17. W F Egelhoff, G G Tibbetts *Solid State Commun.* **29** 53 (1979)
18. M K Bahl, S C Tsai, Y W Chung *Phys. Rev. B, Condens. Matter* **21** 1344 (1980)
19. M G Mason *Phys. Rev. B, Condens. Matter* **27** 748 (1983)
20. M G Mason, in *Cluster Model for Surface and Bulk Phenomena* (New York: Plenum, 1992)
21. V Vijayakrishnan, A Chainani, D D Sarma, C N R Rao *J. Phys. Chem.* **96** 8679 (1992)
22. C N R Rao, V Vijayakrishnan, H N Aiyer, G U Kulkarni, G N Subbanna *J. Phys. Chem.* **97** 11 157 (1993)
23. T L Barr *J. Vac. Sci. Technol. A, Vac. Surf. Films* **7** 1677 (1989)
24. T L Barr *Crit. Rev. Anal. Chem.* **22** 229 (1991)
25. J E Lennard-Jones, R T Goodwin *Proc. R. Soc. London A, Math. Phys. Sci.* **163** 101 (1937)
26. D M Newns *Surf. Sci.* **171** 600 (1986)

27. J-P Ansermet, P-K Wang, C P Slichter, J H Sinfelt *Phys. Rev. B, Condens. Matter* **37** 1417 (1988)
28. S L Rudas, J-P Ansermet, P-K Wang, C P Slichter, J H Sinfelt *Phys. Rev. Lett.* **54** 71 (1985)
29. C D Wagner, in *Practical Surface Analysis* (Eds D Briggs, M P Seach) (New York: Wiley, 1990) p. 595
30. V V Molchanov, V V Chesnokov, R A Buyanov, N A Zaitseva, V N Zaikovskii, L M Plyasova, V N Bukhtiyarov, I P Prosvirin, B N Novgorodov *Kinet. Katal.* **39** 416 (1998) [a]
31. V I Bukhtiyarov, I P Prosvirin, R I Kvon *J. Electron. Spectrosc. Relat. Phenom.* **77** 7 (1996)
32. V I Bukhtiyarov, I P Prosvirin, R I Kvon, S N Goncharova, B S Balzhinimaev *J. Chem. Soc., Faraday Trans.* **93** 2323 (1997)
33. S V Tsybulya, G N Kryukova, S N Goncharova, A N Shmakov, B S Balzhinimaev *J. Catal.* **154** 194 (1995)
34. V M Mastikhin, S N Goncharova, V M Tapilin, V V Terskikh, B S Balzhinimaev *J. Mol. Catal. A, Chem.* **96** 175 (1995)
35. J K Plischke, A J Benesi, M A Vannice *J. Phys. Chem.* **96** 3799 (1992)
36. L V Nosova, M V Stenin, Yu N Nogin, Yu A Ryndin *Appl. Surf. Sci.* **55** 43 (1992)
37. Y Takasu, N Ohashi, X-G Zhang, Y Murakami, H Minagawa, S Sato, K Yahikozawa *Electrochim. Acta* **41** 2595 (1996)
38. M Valden, X Lai, D W Goodman *Science* **281** 1647 (1998)
39. M Che, C O Bennett *Adv. Catal.* **36** 55 (1989)
40. A F Carley, M K Rajumon, M W Roberts *J. Solid State Chem.* **106** 156 (1993)
41. G K Wertheim *Z. Phys. B, Condens. Matter* **66** 53 (1987)
42. G K Wertheim, S B Dicenzo, D N E Buchnan *Phys. Rev. B, Condens. Matter.* **33** 5384 (1986)
43. J J Burton *Catal. Rev. Sci. Eng.* **9** 209 (1974)
44. A A Balandin *Zh. Rus. Fiz.-Khim. O-va* **61** 909 (1929)
45. J Siera, F Rutten, B E Nieuwenhuys *Catal. Today* **10** 353 (1991)
46. M Grunze, in *Fundamental Studies of Heterogeneous Catalysis. The Chemical Physics of Solid Surfaces and Heterogeneous Catalysis* Vol. 4 (Amsterdam: Elsevier, 1982) p. 27
47. F Zaera, J Liu, G Xu, H Kuiper, J Segner *J. Chem. Phys.* **106** 4204 (1997)
48. G L Kellogg *Phys. Rev. Lett.* **55** 2168 (1985)
49. G L Kellogg *Surf. Sci.* **290** 295 (1993)
50. M Eiswirth, G Ertl *Surf. Sci.* **177** 90 (1986)
51. M Sander, R Imbihl, G Ertl *J. Chem. Phys.* **97** 5193 (1992)
52. K Kischer, M Eiswirth, G Ertl *J. Chem. Phys.* **96** 9161 (1992)
53. K Kischer, M Eiswirth, G Ertl *J. Chem. Phys.* **97** 307 (1992)
54. M M Slinko, N I Jaeger *Oscillating Heterogeneous Catalytic Systems* Vol. 86 (Amsterdam: Elsevier, 1994) p. 393
55. N Gottschalk, F Mertens, M Bar, M Eiswirth, R Imbihl *Phys. Rev. Lett.* **73** 3483 (1994)
56. F Mertens, N Cottschalk, M Bar, M Eiswirth, A Mikhailov *Phys. Rev. A, Gen. Phys., Ser. 3* **51** R5193 (1995)
57. F Mertens, R Imbihl *Surf. Sci.* **347** 355 (1996)
58. F Mertens, S Schwegmann, R Imbihl *J. Chem. Phys.* **106** 4319 (1997)
59. P W Murray, G Thornton, M Bowker, V R Dhanak, A Baraldi, R Rosei, M Kiskinova *Phys. Rev. Lett.* **71** 4369 (1993)
60. O M Poltorak *Lektsii po Teorii Geterogennogo Kataliza* (Lectures on the Theory of Heterogeneous Catalysis) (Moscow: Moscow State University, 1968)
61. N I Kobozev *Zh. Fiz. Khim.* **13** 1 (1939) [b]
62. G K Boreskov *Geterogennyi Kataliz v Khimicheskoi Promyshlennosti* (Heterogeneous Catalysis in Chemical Industry) (Moscow: Goskhimizdat, 1955) p. 5
63. V S Chesalova, G K Boreskov *Zh. Fiz. Khim.* **30** 2560 (1956) [b]
64. M Boudart, A Aldag, J E Benson, N A Dougharty, C Girvin *J. Catal.* **6** 92 (1966)
65. M Boudart *Adv. Catal.* **20** 153 (1969)
66. O M Poltorak, V S Boronin *Zh. Fiz. Khim.* **40** 2671 (1966) [b]
67. R van Hardeveld, F Hartog *Surf. Sci.* **15** 189 (1969)
68. R van Hardeveld, F Hartog *Adv. Catal.* **22** 75 (1972)
69. G C Bond, in *Proceedings of the 4th International Congress on Catalysis, Moscow, 1968* Vol. 2, p. 266
70. J F Hamilton, P C Logel *J. Catal.* **29** 253 (1973)
71. J F Hamilton, R C Baetzold *Science* **205** 1213 (1979)
72. G C Bond *Surf. Sci.* **156** 966 (1985)
73. V Ponec *Adv. Catal.* **32** 149 (1983)
74. R Burch *Catalysis* **7** 149 (1985)
75. *Proceedings of International Symposium on the Physics and Chemistry of Finite Systems: from Clusters to Crystals, Richmond, 1991* 105 p.
76. S N Goncharova, E A Paukshtis, B S Balzhinimaev *Appl. Catal.* **126** 67 (1995)
77. Z Xu, F-S Xiao, S K Purnell, O Alexeev, S Kawi, S E Deutsch, B C Gates *Nature (London)* **372** 346 (1994)
78. S Kawi, J-R Chang, B C Gates *J. Phys. Chem.* **98** 12 978 (1994)
79. S Ladas, H Poppa, M Boudart *Surf. Sci.* **102** 151 (1981)
80. F Rumpf, H Poppa, M Boudart *Langmuir* **4** 722 (1988)
81. M Herskowitz, R Holliday, M B Cutlip, C N Kenney *J. Catal.* **74** 408 (1982)
82. S H Oh, C C Eickel *J. Catal.* **128** 526 (1991)
83. T Engel, G Ertl *J. Chem. Phys.* **69** 1267 (1978)
84. T Engel, G Ertl *Adv. Catal.* **22** 2 (1979)
85. V I Savchenko *Usp. Khim.* **55** 462 (1986) [*Russ. Chem. Rev.* **55** 222 (1986)]
86. C T Campbell, S-K Shi, J M White *Appl. Surf. Sci.* **2** 382 (1979)
87. I Stara, V Matolin *Surf. Sci.* **313** 99 (1994)
88. E Gillet, S Channakhone, V Matolin, M Gillet *Surf. Sci.* **152**/**153** 603 (1985)
89. E I Altman, R J Gorte *Surf. Sci.* **172** 71 (1986)
90. D L Doering, H Poppa, J T Dickinson *J. Vac. Sci. Technol.* **20** 827 (1982)
91. E I Altman, R J Gorte *Surf. Sci.* **195** 392 (1988)
92. E I Altman, R J Gorte *J. Catal.* **113** 185 (1988)
93. B Tardy, C Noupa, C Leclercq, J C Bertolini, A Hoareau, M Treilleux, J P Faure, G Nihoul *J. Catal.* **129** 1 (1991)
94. P Briot, A Auroux, D Jones, M Primet *Appl. Catal.* **59** 141 (1990)
95. R W McCabe, L D Schmidt *Surf. Sci.* **66** 101 (1977)
96. P Hofman, S R Bare, D A King *Surf. Sci.* **117** 245 (1982)
97. C S Ko, R J Gorte *J. Catal.* **90** 59 (1984)
98. R J Baird, R C Ku, P Wynblatt *Surf. Sci.* **97** 346 (1980)
99. T W Root, L D Shmidt, G B Fisher *Surf. Sci.* **150** 173 (1985)
100. A K Santra, S Ghosh, C N R Rao *Langmuir* **10** 3937 (1994)
101. P Chou, M A Vannice *J. Catal.* **105** 342 (1987)
102. C N R Rao, V Vijayakrishnan, A K Santra, M W J Prins *Angew. Chem., Int. Ed. Engl.* **31** 1062 (1992)
103. X Xu, D W Goodman *Catal. Lett.* **24** 31 (1994)
104. W K Kuhn, J Szanyi, D W Goodman *Surf. Sci.* **274** L611 (1992)
105. A Ortega, F M Hoffman, A M Bradshaw *Surf. Sci.* **119** 79 (1982)
106. V I Bukhtiyarov, A F Carley, L A Dollard, M W Roberts *Surf. Sci.* **381** L605 (1997)
107. V I Savchenko, G K Boreskov *Kinet. Katal.* **9** 142 (1968) [a]
108. K Christmann, O Schober, G Ertl, M Neumann *J. Chem. Phys.* **60** 4528 (1974)
109. V I Bukhtiyarov, A I Boronin, I P Prosvirin, V I Savchenko *J. Catal.* **150** 262 (1994)
110. V I Bukhtiyarov, I P Prosvirin, R I Kvon *Surf. Sci.* **320** L47 (1994)
111. X E Verykios, F P Stein, R W Coughlin *J. Catal.* **66** 368 (1980)
112. T Mallat, S Frauchiger, P J Kooyman, M Schürch, A Baiker *Catal. Lett.* **63** 121 (1999)
113. A Feller, M Claeys, E van Steen *J. Catal.* **185** 120 (1999)
114. P Denton, A Giroir-Fendler, H Praliaud, M Primet *J. Catal.* **189** 410 (2000)
115. A A Khassin, T M Yurieva, V N Parmon *React. Kinet. Catal. Lett.* **64** 55 (1998)
116. M Nagai, K Koizumi, S Omi *Sekiyu Gakkaishi* **42** 12 (1999)
117. F Haga, T Nakajima, K Yamashita, S Mishima *Nippon Kagaku Kaishi* (11) 758 (1997)
118. D C Koningsberger, J de Graaf, B L Mojet, D E Ramaker, J T Miller *Appl. Catal. A* **191** 205 (2000)
119. M Haruta, N Yamada, T Kobayashi, S Iijima *J. Catal.* **115** 301 (1989)
120. F Boccuzzi, A C Chiorino, S Tsubota, M Haruta *Catal. Lett.* **29** 225 (1994)
121. M Haruta *Catal. Today* **36** 153 (1997)
122. M Okumura, S Nakamura, S Tsubota, T Nakamura, M Azuma, M Haruta *Catal. Lett.* **51** 53 (1998)
123. M Valden, S Pak, X Lai, D W Goodman *Catal. Lett.* **56** 7 (1998)
124. J-D Grunwaldt, C Kiener, C Wögerbauer, A Baiker *J. Catal.* **181** 223 (1999)
125. J -D Grunwaldt, M Maciejewski, O S Becker, P Fabrizioli, A Baiker *J. Catal.* **186** 458 (1999)

126. K Ruth, M Hayes, R Burch, S Tsubota, M Haruta *Appl. Catal. B* **24** L133 (2000)
127. P A Sermon, G C Bond *J. Chem. Soc., Faraday Trans. 1* **74** 385 (1978)
128. M Shibata, N Kawata, T Masumoto, M Kimura, in *Proceedings of Japanese-France Seminar on Catalysis, Tokyo, 1987* p. 98
129. A Baiker, M Kilo, M Maciejewski, S Menzi, A Wokaun, in *New Frontiers in Catalysis* (Amsterdam: Elsevier, 1993) p. 1257
130. A Ueda, M Haruta *Appl. Catal. B* **18** 115 (1998)
131. J J M Schwartz, L D Schmidt *J. Catal.* **148** 22 (1994)
132. A Torncrona, M Skoglundh, P Thormahlen, E Fridell, E Jobson *Appl. Catal. B* **14** 131 (1997)
133. A E Hamdaoui, G Bergeret, J Massardier, M Primet, A Renouprez *J. Catal.* **148** 47 (1994)
134. T Hayashi, M Haruta *Shokubai* **37** 72 (1995)
135. T Hayashi, K Tanaka, M Haruta *J. Catal.* **178** 566 (1998)
136. S Naito, M Tanimoto *J. Chem. Soc., Chem. Commun.* 832 (1988)
137. G C Lane, F S Madica, J T Miller *J. Catal.* **129** 145 (1991)
138. E Mielczarski, S B Hong, R J Davis, M E Davis *J. Catal.* **134** 359 (1992)
139. M G Slin'ko *Modelirovanie Khimicheskikh Reaktorov* (Modelling of Chemical Reactors) (Moscow: Nauka, 1968)
140. *Plenarnye Lektsii Konferentsii po Khimicheskim Reaktoram* (Plenary Lectures of the Conference on Chemical Reactors) (Novosibirsk: Institute of Catalysis, Siberian Branch of the Russian Academy of Sciences, 1996) 179 p.
141. M G Slin'ko, G G Elenin *Khim. Promst* (4) 243 (1989)
142. G G Elenin, M G Slin'ko *Matematicheskoe Modelirovanie Yavlenii na Poverkhnosti (Ser. Matematika i Kibernetika)* [Mathematical Modelling of Surface Phenomena (Mathematics and Cybernetics Series)] (Moscow: Znanie, 1988) No. 8
143. A A Samarskii, M G Slin'ko *Izv. Akad. Nauk, Ser. Khim.* 1895 (1998) [c]
144. T I Zelenyak, M G Slin'ko *Kinet. Katal.* **18** 1235 (1977) [a]
145. T I Zelenyak, M G Slin'ko *Kinet. Katal.* **18** 1548 (1977) [a]
146. M G Slin'ko, T I Zelenyak, T A Akramov, M M Lavrent'ev Jr., V S Sheplev *Matemat. Model.* **9** 87 (1997)
147. L Furuoga, T Shirasaki *Sekiyu Gakkaishi* **13** 1 (1971)
148. Y Wakayama, S-I Tanaka *Surf. Sci.* **420** 190 (1999)
149. P Ehrburger *Adv. Colloid Interface Sci.* **21** 275 (1984)
150. G Schmid *Endeavour, New Ser.* **14** 172 (1990)
151. J D Aiken III, R G Finke *J. Mol. Catal. A* **145** 1 (1999)
152. M A Watzky, R G Finke *Chem. Mater.* **9** 3083 (1997)
153. M A Watzky, R G Finke *J. Am. Chem. Soc.* **119** 10382 (1997)
154. J D Aiken, R G Finke *Chem. Mater.* **11** 1035 (1999)
155. R J Hunter *Foundations of Colloid Science* Vol. 1 (London: Oxford University Press, 198)7
156. A J Bard, L R Faulkner *Electrochemical Methods* (New York: Wiley, 1980)
157. D H Napper *Polymeric Stabilisation of Colloidal Dispersions* (London: Academic Press, 1983)
158. Y Lin, R G Finke *J. Am. Chem. Soc.* **116** 8335 (1994)
159. G Schmid, R Boese, R Pfeil, F Bandermann, S Meyer, G H M Calis, J A W van der Velden *Chem. Ber.* **114** 3634 (1981)
160. G Schmid *Struct. Bonding* **62** 51 (1985)
161. G Schmid *Polyhedron* **7** 2321 (1988)
162. G Schmid, B Morum, J-O Malm *Angew. Chem., Int. Ed. Engl.* **28** 778 (1989)
163. G Schmid *Mater. Chem. Phys.* **29** 133 (1991)
164. G Schmid *Chem. Rev.* **92** 1709 (1992)
165. G Schmid, V Maihack, F Lantermann, S Peschel *J. Chem. Soc., Dalton Trans.* 589 (1996)
166. M N Vargaftik, V P Zagorodnikov, I P Stolyarov, I I Moiseev, V A Likholobov, D I Kochubey, A L Chuvilin, V I Zaikovsky, K I Zamaraev, G I Timofeeva *J. Chem. Soc., Chem. Commun.* 937 (1985)
167. Y Lin, R G Finke *Inorg. Chem.* **33** 4891 (1994)
168. H Bönnemann, G Braun, W Brijoux, R Brinkmann, A S Tilling, K Seevogel, K Siepen *J. Organomet. Chem.* **520** 143 (1996)
169. H Bönnemann, G A Braun *Angew. Chem., Int. Ed. Engl.* **35** 1992 (1996)
170. J Stein, L N Lewis, Y Gao, R A Scott *J. Am. Chem. Soc.* **121** 3693 (1999)
171. J P Wilcoxon, T Martino, E Klavetter, A P Sylwester *Nanophase Mater.* 771 (1994)
172. T J Scmidt, M Noeske, H A Gasteiger, R J Behm, P Britz, W Brijoux, H Bönnemann *Langmuir* **13** 2591 (1997)
173. M T Reetz, R Breinbauer, P Wedemann, P Binger *Tetrahedron* **54** 1233 (1998)
174. Vision 2020 Catalysis Report; http://www ccrhq org/vision
175. H Bönnemann, W Brijoux, A S Tilling, K Siepen *Top. Catal.* **4** 217 (1997)
176. H Bönnemann, G A Braun *Chem. Eur. J.* **3** 1200 (1997)
177. US P. 3 442 973 (1969)
178. J H Sinfelt *Bimetallic Catalysts. Discoveries, Concepts and Applications* (New York: Wiley, 1983)
179. W M H Sachtler *Le vide* **163** 19 (1979)
180. S N Augustine, W M H Sachtler *J. Phys. Chem.* **91** 5953 (1987)
181. Y Y Huang, W M H Sachtler *J. Catal.* **188** 215 (1999)
182. M Bonarowska, A Malinowski, Z Karpiński *Appl. Catal. A* **188** 145 (1999)
183. US P. 3 617 518 (1971)
184. G Diaz, A Gomezcortes, M Benaisa *Catal. Lett.* **38** 63 (1996)
185. C P Shao, L Fan, K Fujimoto, Y Iwasawa *Appl. Catal. A* **128** L1 (1995)
186. C T Campbell, in *Handbook of Heterogeneous Catalysis* Vol. 2 (Eds G Ertl, H Knozinger, J Weitkamp) (Weinheim: VCH, 1997) p. 814
187. W M H Sachtler, in *Handbook of Heterogeneous Catalysis* Vol. 3 (Eds G Ertl, H Knozinger, J Weitkamp) (Weinheim: VCH, 1997) p. 1077
188. H-W Yang, J C Lin, T Engel *Surf. Sci.* **289** 267 (1993)
189. J A Rodrigues, R A Campbell, D W Goodman *J. Vac. Sci. Technol. A, Vac. Surf. Films* **10** 2540 (1992)
190. A Sellidj, B E Koel *Surf. Sci.* **284** 139 (1993)
191. M W Ruckman, M Strongin *Phys. Rev. Lett.* **29** 7105 (1984)
192. U Schneider, H Busse, R Linke, G R Castro, K Wandelt *J. Vac. Sci. Technol. A, Vac. Surf. Films* **12** 2069 (1994)
193. G R Castro, U Schneider, H Busse, T Janssens, K Wandelt *Surf. Sci.* **269**/**270** 321 (1992)
194. C Xu, B E Koel *Surf. Sci.* **310** 198 (1994)
195. E Garfunkel, M Yu, S Yang, X Feng *J. Vac. Sci. Technol. A, Vac. Surf. Films* **7** 1579 (1989)
196. X H Feng, M R Yu, S Yang, G Meigs, E Garfunkel *J. Chem. Phys.* **90** 7516 (1989)
197. F Besenbacher, I Chorkendorff, B S Clausen, B Hammer, A M Molenbroek, J K Nørskov, I Stensgaard *Science* **279** 1913 (1998)
198. N Toshima, T Yonezawa *New J. Chem.* 1179 (1998)
199. N Toshima, M Harada, T Yonezawa, K Kushihashi, K Asakura *J. Phys. Chem.* **95** 7448 (1991)
200. N Toshima, K Kushihashi, T Yonezawa, H Hirai *Chem. Lett.* 1769 (1989)
201. N Toshima, T Yonezawa, M Harada, K Asakura, Y Iwasawa *Chem. Lett.* 815 (1990)
202. T Yonezawa, N Toshima *J. Chem. Soc., Faraday Trans.* **91** 4111 (1995)
203. N Toshima, M Harada, Y Yamazaki, K Asakura *J. Phys. Chem.* **96** 9927 (1992)
204. M Harada, K Asakura, N Toshima *J. Phys. Chem.* **98** 2653 (1994)
205. K Asakura, Y Yamazaki, H Kuroda, M Harada, N Toshima *Jpn. J. Appl. Phys.* **32** 448 (1993)
206. N Toshima, Y Wang *Adv. Mater.* **6** 245 (1994)
207. T E Hoost, G W Graham, M Shefel, O Alexeev, B C Gates *Catal. Lett.* **38** 57 (1996)

[a] — *Kinet. Catal. (Engl. Transl.)*
[b] — *Russ. J. Phys. Chem. (Engl. Transl.)*
[c] — *Russ. Chem. Bull. (Engl. Transl.)*